Comparative study of MIMO control methodologies for vibration reduction in Self-Sensing multi-piezoelectric systems

Halim Ould Lahsen, Julien Huillery, Anton Korniienko, Fabien Mieyeville

Comparative study of MIMO control methodologies for vibration reduction in Self-Sensing multi-piezoelectric systems

Halim OULD LAHSEN, Anton KORNIIENKO, Julien HUILLERY, Fabien MIEYEVILLE,[†‡]

Abstract

This work addresses the challenge of vibration control in a flexible plate using two piezoelectric patches in a Self-Sensing Actuator (SSA) configuration, meaning they simultaneously serve as sensors and actuators. Two H_∞ MIMO control strategies, centralized and structured, are developed and compared, accounting for the coupling effects between the piezoelectric elements. Additionally, a third strategy based on a previously developed SISO methodology is also included for comparative analysis. The identification-based modeling approach coupled with model reduction techniques enable the design of a low-order controller, achieving significant vibration reduction within a specified frequency range.

Keywords: H_∞ control, centralized control, structured control, Self-Sensing Actuator, piezoelectric actuation, flexible structure, vibration control.

1 Introduction

Ambient vibrations represent a significant class of challenges to address in various industrial applications, particularly in the fields of automotive, aerospace, and robotics, see [3, 9, 16, 13, 14]. These vibrations degrade system performance, accelerate failures, and can lead to severe malfunctions or complete loss of functionality.

Recent advances in active control have enabled the development of effective solutions to mitigate these vibrations, [4, 11]. Piezoelectric materials, due to their high performance and rapid response, are widely used in such systems. Their ability to meet stability and reliability requirements makes them essential components in vibration control and numerous studies have demonstrated the effectiveness of these materials in reducing vibrations in flexible systems, [9, 8]. Among the approaches developed, the Self-Sensing Actuator

*This work was supported by French Ministry of Higher Education and Research.

†Halim Ould Lahsen and Fabien Mieyeville are with Univ Lyon, Université Claude Bernard Lyon 1, INSA Lyon, Ecole Centrale de Lyon, CNRS, Ampère, UMR5005, 69622 Villeurbanne, France (e-mail: halim.ould-lahsen@univ-lyon1.fr; fabien.mieyeville@univ-lyon1.fr)

‡Anton Korniienko and Julien Huillery are with Univ Lyon, Ecole Centrale de Lyon, INSA Lyon, Université Claude Bernard Lyon 1, CNRS, Ampère, UMR5005, 69130 Ecully, France (e-mail: anton.korniienko@ec-lyon.fr; julien.huillery@ec-lyon.fr)..

(SSA) technique, introduced by [2], employs a single piezoelectric element as both a sensor and an actuator. This method simplifies the control system architecture by eliminating the need for separate sensors and actuators, thereby reducing costs and enhancing overall reliability.

In our previous work [7] under publication, a robust H_∞ control methodology was applied to a SISO system, demonstrating the effectiveness of local vibration reduction with a single SSA piezoelectric element. In the present work, we extend this methodology to a MIMO system with two SSA piezoelectric elements, taking into account the coupling between the two piezoelectric elements and allowing to address more global vibration reduction objectives. Since most of the methodological aspects were developed in our previous work [7], here we focus more on practical questions and mainly on the possibility of decentralized control design and implementation.

We adopt an approach for model identification, where each transfer function is identified separately, taking into account the modal similarities of the piezoelectric elements. Once the MIMO system model is obtained, its order is reduced according to the original idea of [11]. Then, two control strategies based on H_∞ synthesis are developed: centralized and structured control, where specific constraints are imposed on the controller structure. The methodology emphasizes the importance of structured control, where the design ensures that each piezoelectric element is controlled by an independent local controller. While centralized control is also considered for benchmarking purposes, the primary focus is on achieving decentralized control that respects the structural constraints of the system. In addition, the controllers are designed to impose roll-off characteristics outside the frequency range of interest. This ensures a reduction of the control signal's power and improves robustness as well as measurement noise filtering. Simulations and experimental results illustrate the effectiveness of the proposed control design methodology.

Notations: In this work we denote $G_{x\to y}$ and $T_{x\to y}$ respectively the open-loop and closed-loop transfer function from signal x to signal y, Throughout the study, the system is assumed to be a Linear Time-Invariant (LTI) system, allowing all computations to be performed in the Laplace domain. Temporal signals are represented in lowercase (e.g., v_s, v_c), while Laplace-domain signals are represented in uppercase (e.g., V_s, V_c).

2 Experimental bench

A suspended $33 \times 33\ cm^2$ flexible plate equipped with two piezoelectric patches is used for experimental illustration of the vibration control solution proposed. Fig. 1 and 2 provide a schematic representation and photos of the experimental setup.

The vibrations of the flexible plate are induced by applying an excitation signal v_{exc} to the "Data Physics" "M20/PA300E" shaker which in turn applies a disturbing force at a specific excitation point on the plate. The excitation signal v_{exc} is generated by the "DS 1104 R&D" controller card and amplified by a "Data Physics" $30W$ power amplifier. The vibrations of the plate are measured by two identical piezoelectric elements (PE_1 and PE_2) "DuraACT P-876.A15" by "PI Ceramic" with internal capacitances $C_p^{PE_1} \approx C_p^{PE_2} \approx 37\,nF$. As depicted in Fig. 1, the two measured signals v_{PE_1} and v_{PE_2} are passed to the two SSA balancing bridges (one for each piezoelectric element) before reaching the controller. In return, the controller computes the control signals v_{c_1} and v_{c_2} applied to the piezoelectric elements through the SSA balancing bridges. With-

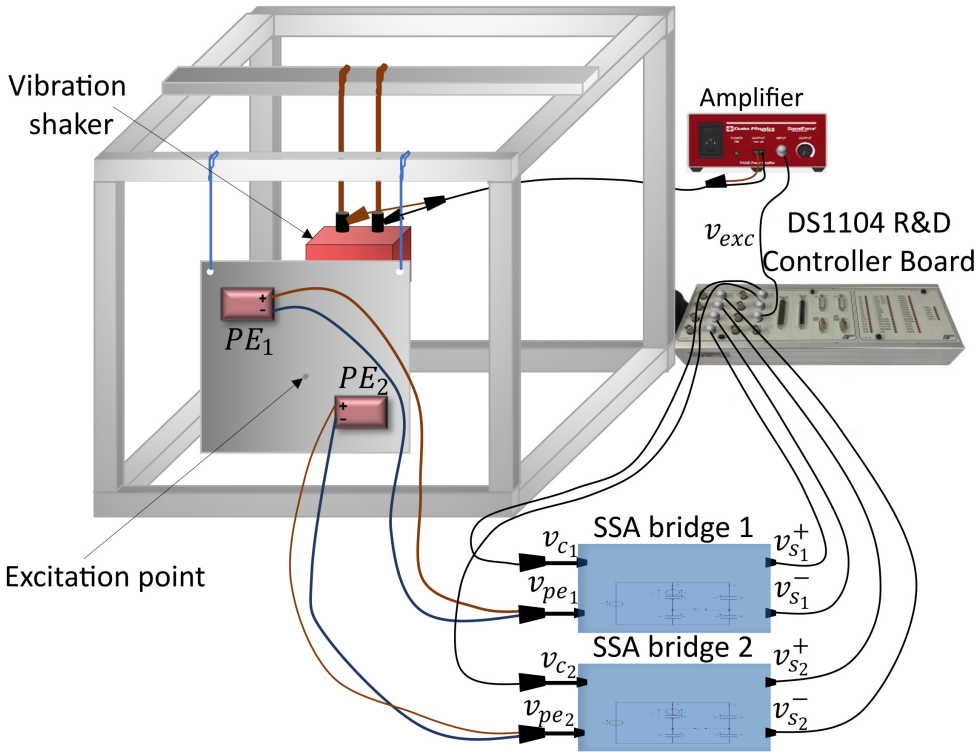

Figure 1: Experimental setup for active vibration control with Self-Sensing Actuators.

out these circuits, the actuation signal and the detection signal share the same terminals, creating a direct coupling that introduces additional noise, thus disrupting the control by reducing the signal-to-noise ratio. The balancing bridges separate these signals, reducing interference and improving the signal-to-noise ratio. Additionally, digital compensation is also performed to optimize the system's performance. Further details about the SSA implementation and modelling used in this work can be found in [7].

The vibrations of the plate exhibit its most significant power spectral density level in the frequency range $\Omega = [200; 300]$Hz. This frequency band Ω is thus selected for control purpose as it includes the plate's most energetic vibration modes.

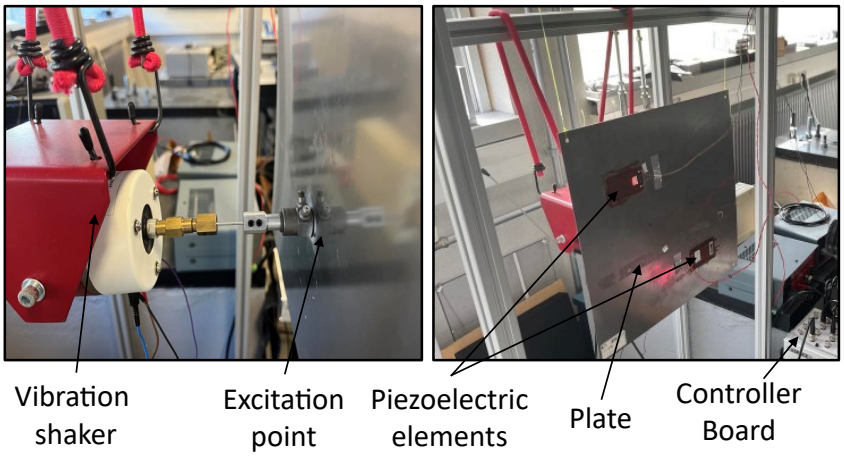

Figure 2: Photos of the experimental bench.

3 Identification and model reduction

The overall process of system modeling, order reduction, and control synthesis is summarized in Fig. 3. The goal is to obtain a decentralized, robust reduced-order controller that decreases the system vibrations in the frequency band Ω without spillover effects. The approach used was initially proposed in [11] and specialized to the SSA configuration in our work under publication [7]. In this work, we focus only on new aspects of the work necessary to address the decentralized nature of the controller required for implementation simplification. The interested reader is invited to consult the details on H_∞ criteria, digital controller implementation, and SSA direct term compensation in [11] and [7]. This section presents identification techniques used to build a model of the instrumented flexible plate, along with model reduction methods used to simplify the system representation while preserving relevant dynamics for control.

The proposed modeling procedure is based on system black-box identification [5]. Even though the subspace based identification can be used to directly obtain the MIMO state space representation of the system, in this work we opted for SISO by SISO polynomial transfer function identification based on prediction error methods. This approach appears to be more numerically stable and allows, together with the nominal transfer function, to estimate the size of the uncertainty due to the noise and time-limited identification experiment. The increase in model order caused by the separate identification of each transfer function is compensated by the proposed pole selection procedure, as explained later.

3.1 Input-output and system definitions

The system to be controlled involves three input signals: the excitation signal v_{exc} and two control signals $v_{c_{1,2}}$. The excitation signal v_{exc} is applied to induce vibrations in the plate, while the control signals $v_{c_{1,2}}$ are applied to the piezoelectric elements through the SSA balancing bridges. In response to these inputs, the system produces two output signals $v_{s_{1,2}}$, which are the measures from the two piezoelectric elements through the SSA balancing bridges, see Fig. 1. The behavior of the MIMO system to be controlled can thus be described in the Laplace domain by the following equation:

$$\begin{bmatrix} V_{s_1} \\ V_{s_2} \end{bmatrix} = \overbrace{\begin{bmatrix} G_{V_{exc}\to V_{s_1}} & G_{V_{c_1}\to V_{s_1}} & G_{V_{c_2}\to V_{s_1}} \\ G_{V_{exc}\to V_{s_2}} & G_{V_{c_1}\to V_{s_2}} & G_{V_{c_2}\to V_{s_2}} \end{bmatrix}}^{G(s)} \begin{bmatrix} V_{\text{exc}} \\ V_{c_1} \\ V_{c_2} \end{bmatrix} \tag{1}$$

where V_{c_1} and V_{c_2} are the control signals in Laplace domain applied to PE_1 and PE_2, respectively, and V_{s_1} and V_{s_2} are the output signals measured from the corresponding piezoelectric elements connected to the SSA balancing bridges.

3.2 Identification steps

Black-box identification approaches rely on collecting experimental measurements and processing the input-output signals to estimate the parameters of a transfer function whose structure is given. In this work, the ARX (AutoRegressive with eXogenous input) model structure combined with the prediction error method [5] is adopted. The ARX structure

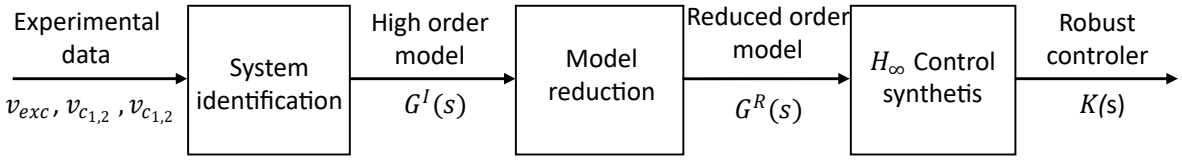

Figure 3: Proposed Control design methodology

is preferred for its explicit parameter estimation formulas and superior numerical stability, as established in [6] and widely applied in industrial settings [15].

A trade-off has to be made in the choice of the model order. It should be high enough to capture the important dynamics of the system, but not so high as to avoid overfitting the measurement noise, which would introduce excessive uncertainties. In this work, Akaike's Information Criterion [5] is used for order selection. Moreover, the model order can further be reduced by adding a second step to the identification process: the first step classically involves using the experimental data to build a high-order ARX model. In the second step, noiseless simulated data is generated through temporal simulations of the first identified model and then used to estimate a new lower-order ARX model, denoted $G^I(s)$ (see Fig. 3).

3.3 Model order reduction

The order of the initially identified model $G^I(s)$ remains too high with respect to the control objectives and could lead to the design of an unnecessarily complex high order controller. To address this, the model order reduction method based on Modal Form Truncation (MFT) introduced in [10] is used to eliminate the irrelevant poles outside the frequency band of interest $\Omega = [200; 300]$Hz. However, MFT generally introduces errors between the original model, $G^I(s)$, and its truncated counterpart, $G^T(s)$, especially around the locations of zeros. To mitigate this problem, as discussed in [12, 7], the optimization step involves adjusting the zeros of $G^T(s)$ to minimize the relative error between the original model, $G^I(s)$, and the optimized version,

Another key aspect of the proposed system identification is the poles selection procedure. This is particularly relevant in polynomial identification, where transfer functions are estimated individually for each input-output pair. Indeed, since they are influenced by the same vibration modes of the plate, these transfer functions theoretically share common poles. However, if the identification process is conducted separately for each transfer function, the estimated poles are not exactly identical but rather close to each other. Blind concatenation of the identified transfer function would result in an overly high order MIMO system model. To avoid this, we propose to select and fix the common poles between the identified transfer functions.

Let $G_i^O(s)$, with $i = 1, \ldots, 6$, be the transfer functions associated with each input-output pairs of (1). Each transfer function has poles $p_{i,j}$, where i is the index of the transfer function and j is the index of the pole. The poles are compared between the different transfer functions. They are considered to be close if the difference between them is less than a threshold $\epsilon_p = 2\pi \times 0.5$:

$$\max_{k,l} \|p_{i,k} - p_{i,l}\| < \epsilon_p \tag{2}$$

Once the closest poles are identified, their average position is computed by taking the

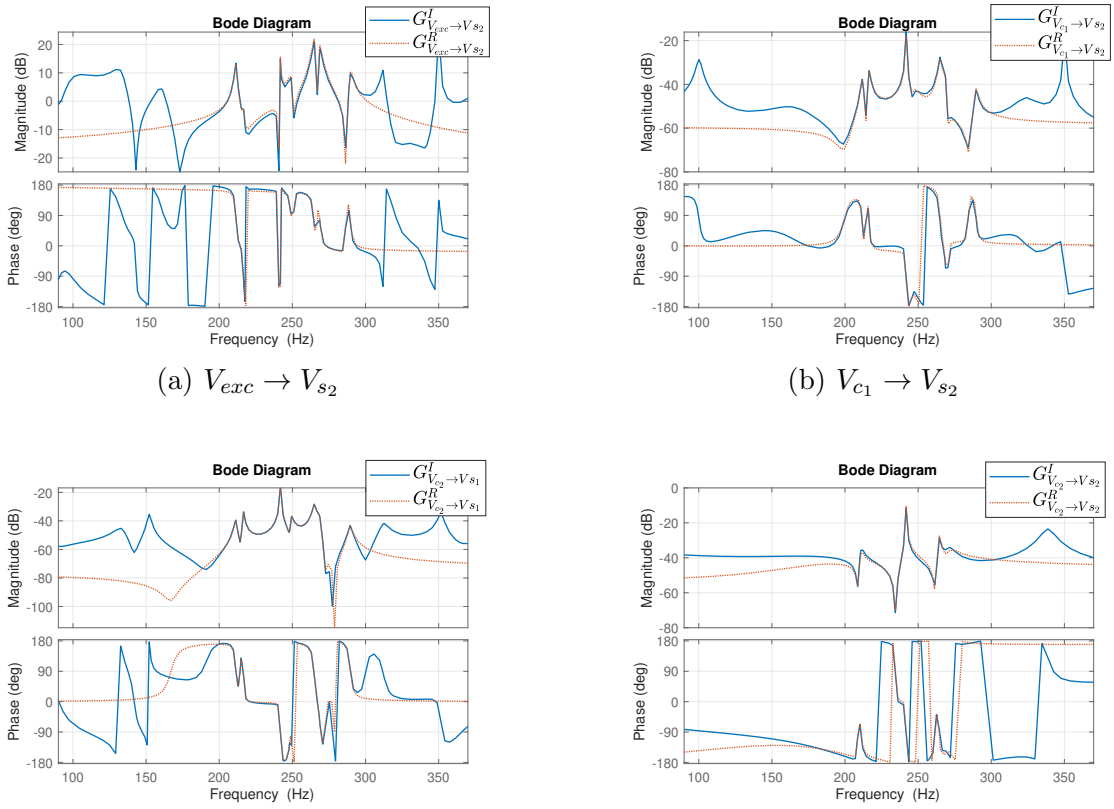

(a) $V_{exc} \to V_{s_2}$ (b) $V_{c_1} \to V_{s_2}$

(c) $V_{c_2} \to V_{s_1}$ (d) $V_{c_2} \to V_{s_2}$

Figure 4: Identified models $G^I_{x\to y}$ (solid blue lines) and reduced-order models $G^R_{x\to y}$(dashed red lines).

average of the real and imaginary parts:

$$\bar{p}_j = \frac{1}{n}\sum_{i=1}^{n} p_{i,j} \tag{3}$$

This provides an average value for each pole j, which is used to adjust the poles in all transfer functions. This method ensures the consistency of the poles across the transfer functions $G^R_i(s)$ and improves the accuracy of the overall model. The overall reduced model obtained after this pole selection procedure is denoted as $G^R(s)$.

To validate the modeling process, Figure 4 illustrates the initial identified models $G^I_i(s)$ and the reduced models $G^R_i(s)$ for selected transfer functions of the global MIMO model. This visual comparison highlights the consistency between the initial and reduced models and demonstrates the effectiveness of the reduction process in preserving the key dynamic behavior of the system while simplifying its representation.

Please note, that the difference between this reduced order model $G^R(s)$ and initially identified high order model $G^I(s)$ is taken into account in control design similarly to the model reduction uncertainty as detailed in [7].

4 Control strategies

In this section, we describe each approach based on the type of control and the methodologies derived from the schematic presented in Figure 5. Specifically, the SISO, MIMO centralized, and MIMO structured approaches are introduced with a focus on their respective principles and design characteristics.

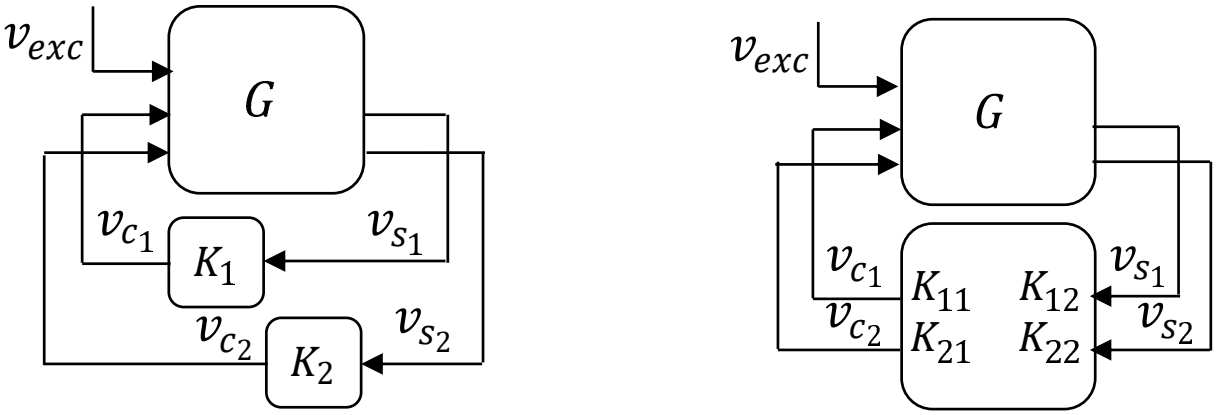

Figure 5: Comparison of SISO and MIMO control strategies in the system configuration for vibration control with two piezoelectric elements. (a) SISO, (b) MIMO.

4.1 Independant SISO design

In the Independent SISO approach, each piezoelectric element is treated as a separate system and its control is designed independently thanks to the H_∞ design procedure without considering coupling effects exactly as proposed in [7]. This method assumes no interaction between the two piezoelectric elements. The design of two controllers $K_1(s)$ and $K_2(s)$ is performed separately, which simplifies the design but ignores couplings between the elements.

4.2 Centralized MIMO design

In the MIMO centralized approach, the interactions (or couplings) between multiple inputs and outputs are explicitly modeled and accounted for during controller design. Here, a single global controller is designed for the entire system, represented by a 2x2 matrix as illustrated in Figure. 5b:

$$K^C(s) = \begin{bmatrix} K_{11}(s) & K_{12}(s) \\ K_{21}(s) & K_{22}(s) \end{bmatrix} \tag{4}$$

where $K_{ij}(s)$ are the controller transfer functions for each input-output pair. The H_∞ criteria proposed in [7] is extended and applied to our system with two control inputs V_{c_1}, V_{c_2} and two measurement outputs V_{s_1}, V_{s_2}, see also [11].

This method has the potential to achieve the best performance by using the overall system model, including all couplings. However, the high computational complexity and implementation cost make it impractical for systems with many piezoelectric elements.

4.3 Structured MIMO design

In the structured (or decentralized) MIMO approach, we aim to achieve the benefits of the MIMO centralized method while maintaining a simpler, diagonal controller structure. The structure of the control law is given by:

$$K^S(s) = \begin{bmatrix} K_{11}(s) & 0 \\ 0 & K_{22}(s) \end{bmatrix} \tag{5}$$

Here, the diagonal structure implies that each piezoelectric element is controlled independently by its respective controller, $K_{11}(s)$ or $K_{22}(s)$. However, the synthesis considers the full MIMO model, ensuring that couplings between the elements are accounted for during the design stage.

The MIMO structured methodology can be seen as a special case of the MIMO centralized approach. If no structural constraints are imposed during the synthesis of the structured controller, the solution converges to the centralized controller. However, by imposing the diagonal structure, the implementation complexity is significantly reduced, making this approach scalable to larger systems with many piezoelectric elements.

However, the obtained design problem is a non-convex one since it is associated with the structured H_∞ design. It can be solved [1] provided a good initial guess for the controller is given. In this study, we initialize the structured controller using the independently synthesized $K_1(s)$ and $K_2(s)$ from the SISO methodology. The structured controller matrix is thus initialized as:

$$K_0^S(s) = \begin{bmatrix} K_1(s) & 0 \\ 0 & K_2(s) \end{bmatrix} \tag{6}$$

This initialization takes advantage of the fact that $K_1(s)$ and $K_2(s)$ performed well in simulations and experiments when applied independently. By using these as a starting point, the iterative optimization process converges to a solution $K^S(s)$ that maintains the performance benefits observed in the SISO design when applied to the overall system as explained in the next section.

5 Results and analysis

In order to illustrate the results of the proposed design methodologies, tree simulations and experiments where performed. First is based on the independent SISO design in Figure 5a where only one piezoelectric element is controlled at time (say K_1), putting another controller to zero ($K_2 = 0$). Second and third are implemented according to Figure 5b with controllers $K^C(s)$ and $K^S(s)$ obtained respectively based on Centralized and Structured MIMO H_∞ design.

For the evaluation of simulation and experimental results, measurements of v_{s_i} were performed for each piezoelectric element and used as an indicator of the local dynamic response of the plate. The reduction rate is computed in the time domain using the Root Mean Square (RMS) value of each measurement in open-loop ($v_{s_i}^{OL}$) and closed-loop ($v_{s_i}^{CL}$) configurations:

$$r_{\text{RMS}}^{\text{vib}}(PE_i) = \left(1 - \frac{RMS(v_{s_i}^{CL})}{RMS\left(v_{s_i}^{OL}\right)}\right) 100\% \tag{7}$$

The higher this indicator is for a given piezoelectric element, the better the vibration reduction rate is locally achieved by that piezoelectric element. To evaluate the overall reduction, we decided to compute the common RMS value by simply concatenating the output vectors as follows:

$$r_{\text{RMS}}^{\text{vib}}(PE_1, PE_2) = \left(1 - \frac{RMS\left(\begin{bmatrix} v_{s_1}^{CL} \\ v_{s_2}^{CL} \end{bmatrix} \right)}{RMS\left(\begin{bmatrix} v_{s_1}^{OL} \\ v_{s_2}^{OL} \end{bmatrix} \right)} \right) 100\% \tag{8}$$

Table 1 presents the reduction rates obtained for each control strategy, both for simulation and experimental cases, as well as for each of the two piezoelectric elements (PE_1 and PE_2) separately. Additionally, the average reduction rate for the two elements is also provided to give an overall evaluation of the control strategies' performance.

The results show different level of vibration reduction depending on the selected control strategy.

The SISO PE_1 strategy achieves a significant reduction in PE_1 vibrations in simulation (56%) and experimentation (53.2%), but its effect on PE_2 remains minimal (8% in simulation and only 2.96% in experimentation). This result is not surprising since it indicates a strong selective action on PE_1 with negligible impact on PE_2.

Similarly for the SISO PE_2 strategy which achieves a better reduction level at the PE_2 location. Surprisingly, it shows an asymmetry between simulation and experiment (42.4% vs 28.6%).

The discrepancy may be due to unmodeled effects in the experimental setup. A possible explanation is that PE_2 is located closer to the excitation point, leading to different boundary conditions compared to PE_1, which is more constrained. In both SISO cases however, the common reduction rate is smaller confirming the strong selective action of each piezoelectric element.

The MIMO Centralized strategy leverages the coupling between PE_1 and PE_2, leading to best overall performance. A good level of vibration reduction is obtained for both locations. While the overall reduction reach the best score of 38.8% and 40.5% in simulation and experiment respectively.

The most interesting results are obtained with the MIMO Structured strategy. Despite the fact that a diagonal structure on the controller is imposed, the reduction level is only slightly decreased compared to the MIMO Centralized strategy. This tendency is similar for both local and overall reduction levels.

Additionally the power spectral density (PSD) for the signals v_{s_1} and v_{s_2} in open and closed-loop configurations for MIMO Structured strategy is shown in Fig. 6. The results indicate that the experimental and simulation data exhibit similar peak attenuation levels between open and closed-loop cases across the frequency range Ω. This verifies that the reduced-order model provides an adequate representation of the system dynamics within the specified frequency range. Additionally, stability is maintained, and no spillover effects are observed.

Table 1: Summary table of reduction rates of the control signal for each configuration

Strategy	**Simulation**			**Experimentation**		
	$r^{\text{vib}}_{\text{RMS}}(PE_1)$	$r^{\text{vib}}_{\text{RMS}}(PE_2)$	$r^{\text{vib}}_{\text{RMS}}(PE_1, PE_2)$	$r^{\text{vib}}_{\text{RMS}}(PE_1)$	$r^{\text{vib}}_{\text{RMS}}(PE_2)$	$r^{\text{vib}}_{\text{RMS}}(PE_1, PE_2)$
SISO PE_1	56%	8%	27,5%	53,2%	2,96%	23,76%
SISO PE_2	7%	42,4%	28,5%	11,8%	28,6%	20%
MIMO Centralized	40,1%	37%	38,8%	39,5%	41,5%	40,5%
MIMO Structured	37,22%	35,91%	36,55%	41,8%	33,89%	37,5%

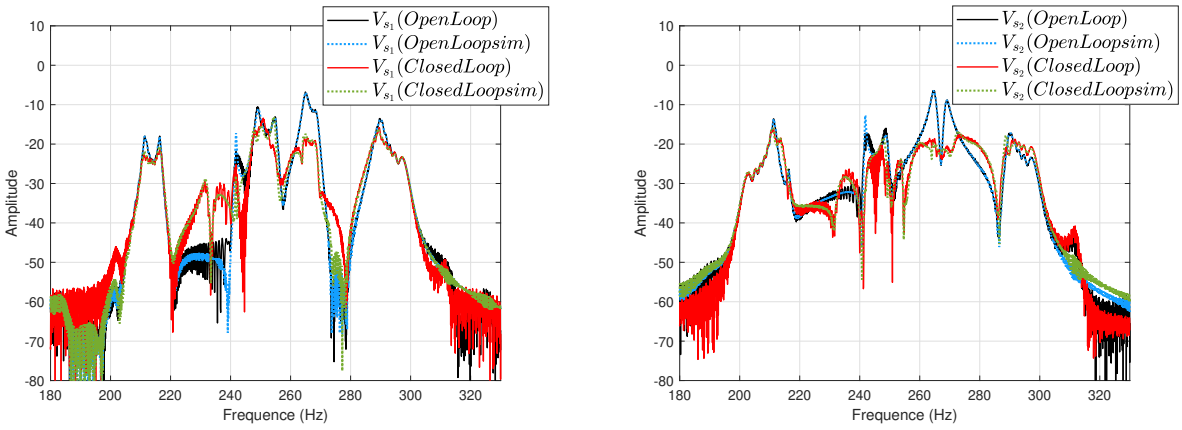

(a) (b)

Figure 6: Power spectral density of the obtained signals: (a) v_{s_1} and (b) v_{s_2}. Experimental Open Loop (black line), experimental Closed Loop (red line), simulated Open Loop (dashed blue line), and simulated Closed Loop (dashed green line).

6 Conclusion and future perspectives

In conclusion, this study demonstrates the effectiveness of advanced control strategies for vibration suppression in a flexible plate using piezoelectric patches in a Self-Sensing Actuator (SSA) configuration. Among the evaluated approaches, the structured H_∞ MIMO control strategy stands out, achieving a notable 40% reduction in vibrations while addressing the coupling effects between the piezoelectric elements. This result highlights the structured strategy's ability to address the trade-off between performance and controller complexity, making it a promising solution for practical applications requiring precise vibration control. Future work could explore the integration of this approach into more complex systems combining more then two sensors/actuators.

References

[1] P. Apkarian and Dominikus Noll. The H∞ Control Problem is Solved. *Aerospace Lab*, (13):pages 1–11, November 2017.

[2] Jeffrey J Dosch, Daniel J Inman, and Ephrahim Garcia. A self-sensing piezoelectric actuator for collocated control. *Journal of Intelligent material systems and Structures*, 3(1):166–185, 1992.

[3] M. R. Kermani, R. V. Patel, and M. Moallem. Multimode control of a large-scale robotic manipulator. *IEEE Transactions on Robotics*, 23(6):1264–1270, 2007.

[4] Joël Bafumba Liseli, Joël Agnus, Philippe Lutz, and Micky Rakotondrabe. An overview of piezoelectric self-sensing actuation for nanopositioning applications: Electrical circuits, displacement, and force estimation. *IEEE Transactions on Instrumentation and Measurement*, 69(1):2–14, 2019.

[5] L. Ljung. *System Identification: Theory for the User*. Prentice Hall PTR, Englewood Cliffs, NJ, 2. edition, 1999.

[6] L. Ljung and B. Wahlberg. Asymptotic properties of the least-squares method for estimating transfer functions and disturbance spectra. *Advances in Applied Probability*, 24(2):412–440, 1992.

[7] Halim Ould Lahsen, Anton Korniienko, Julien Huillery, and Fabien Mieyeville. Active vibration control of smart structures using a single self-sensing piezoelectric actuator. preprint, July 2024.

[8] Farzad Pourboghrat, Harin Pongpairoj, Il-Jin Youn, Ramesh Balasubramaniam, Raghuram Radhakrishnan, Morteza Daneshdoost, and Mohammed R Sayeh. Vibration control of flexible structures using self-sensing actuators. In *Smart Structures and Materials 1999: Smart Structures and Integrated Systems*, volume 3668, pages 950–959. SPIE, 1999.

[9] A. Preumont. *Vibration Control of Active Structures, An Introduction*. Springer Dordrecht, 3rd edition, July 2011.

[10] Madan G Singh and André Titli. Handbook of large-scale systems engineering applications. *IEEE Transactions on Systems, Man, and Cybernetics*, (4):595–595, 1985.

[11] Peng Wang, Anton Korniienko, Xavier Bombois, Manuel Collet, Gérard Scorletti, Ellen Skow, Chuhan Wang, and Kévin Colin. Active vibration control in specific zones of smart structures. *Control Engineering Practice*, 84:305–322, 2019.

[12] Peng Wang, Gerard Scorletti, Anton Korniienko, and Manuel Collet. Multi-variable model reduction of smart structure in active vibration control. volume 51, pages 441–446, 2018.

[13] K Zhang, G. Scorletti, M. Ichchou, and F. Mieyeville. Quantitative robust linear parameter varying H∞ vibration control of flexible structures for saving the control energy. *Journal of Intelligent Material Systems and Structures*, 26(8):1–22, May 2015.

[14] Xueji Zhang, Zhe Dong, Zhong, Martin Hromcik, Kristian Hengster-Movric, Cassio Faria, Herman D Van der Auweraer, and Wim Desmet. Reduced-order robust controller design for vibration reduction. Technical report, SAE Technical Paper, 2016.

[15] Y. Zhu. *Multivariable system identification for process control*. Elsevier, 2001.

[16] Mateusz Zielinski. *A Distributed Active Vibration Control System Based on the Wireless Sensor Network for Automotive Applications*. PhD thesis, Ecully, Ecole centrale de Lyon, 2015.